Nuclear Instruments and Methods in Physics Research B 96 (1995) 497–507

NIM B
Beam Interactions with Materials & Atoms

ELSEVIER

The transition from quantum to classical atom–surface scattering

J.R. Manson

Department of Physics and Astronomy, Clemson University, Clemson, SC 29634, USA

Abstract

We present a fully quantum mechanical model of atom–surface scattering which can be extended through the correspondence principle to the classical limit. Calculations for comparison with recent He atom scattering experiments on the Cu(001) surface show excellent agreement with the observed diffuse inelastic backgrounds. The temperature dependence of the scattering in the classical regime demonstrates conclusively that the He atoms exchange energy with a vibrating continuum interaction potential due to the surface electron density and not directly with a lattice of surface atomic cores.

1. Introduction

The subject of this paper is a theoretical description of the diffuse inelastic intensity observed in atom–surface scattering experiments at thermal energies. For small mass, low energy atomic projectiles and low surface temperatures, the dominant features resolved in the time-of-flight experimental measurements are sharp intensity features arising from diffraction, diffuse elastic scattering from impurities, and sharp single phonon inelastic peaks due to the exchange of surface localized phonon modes. This is the quantum scattering regime.

At higher projectile energies and large surface temperatures these sharp quantum features are suppressed and only broad inelastic features are observed. This is the characteristic of the classical scattering regime.

We give a brief review of the theory of multiphonon scattering in the quantum regime and then extend this theory into the classical regime, where the result for the scattered intensities can be expressed in terms of simple closed-form expressions. Calculations based on a simple but fully quantum mechanical model of the atom–surface interaction give excellent agreement with recent experiments [1].

The diffuse inelastic background consists of two parts, incoherent inelastic scattering from defects [2] and the coherent multiphonon contribution. For clean, well ordered surfaces the multiphonon contribution usually dominates, and although diffuse, it is not featureless. Structure appears in the multiphonon contribution and peaks can occur which resemble single phonon features [3], thus for this reason alone it is important to have a good understanding of these processes. A good knowledge of the form and shape of the diffuse inelastic signal is essential for background subtraction in order to obtain the true values of the elastic and single surface phonon peaks. However, the inelastic background contains far more interesting physical information than simply that necessary for background subtraction. We will show that it provides important information on the interaction potential which couples the projectile to the surface, and the large range of experimental conditions currently available provide excellent examples of the transition from the quantum mechanical regime to the classical scattering regime.

The scattering of small mass and low energy neutral atoms has for many years been of interest as a method of obtaining information about fundamental physical processes occurring at surfaces. Interest in this field of study was initially sparked by the seminal experiments of Stern and coworkers [4–7] who used a thermal beam of He atoms diffracting from a cleaved LiF(001) surface to verify the De Broglie hypothesis for the wavelike nature of a particle. This work very quickly stimulated a large degree of theoretical interest [8–17], virtually all of which was carried out within the framework of what is now known as the distorted wave Born approximation.

In the late 1960s and early 1970s advances in vacuum technology, and especially the development of extremely monoenergetic molecular jet beams of thermal energy particles, stimulated a new round of experimental activity [18–22] which has continued unabated to the present time. These experiments were quickly followed by renewed theoretical interest [23–25]. More recent experimental and theoretical developments have been discussed in a number of excellent review articles in the last few years [26–33].

The characteristic features of the scattered intensity can be roughly grouped into four components: elastic diffraction peaks arising as a result of the underlying periodicity of the crystal substrate, the diffuse elastic intensity caused by defects, single surface phonon peaks, and the diffuse inelastic background. The elastic diffraction peaks are the easiest to interpret as their positions are determined by the

0168-583X/95/$09.50
SSDI 0168-583X(95)00238-3

periodicity of the crystal surface. The intensities of these diffraction peaks relative to the incident beam, when compared with calculations, give the corrugation of the surface potential as observed by the scattering projectiles. Broadening and shifts in position of the diffraction peaks indicate deviations from perfect periodicity in the surface. The diffuse elastic peak appears at all scattering angles and is due to symmetry-breaking impurities and imperfections on the surface. Its origins are less well understood than the diffraction, although it has been shown to yield important information about the differential cross section of defects [34–36] or adsorbates [37] on the surface. The single phonon peaks arise from single quantum inelastic interactions with phonon modes which are localized in the surface region. These include surface modes associated with a perfect crystal, such as Rayleigh phonons, and also other excitations such as modes due to surface adsorbates. These single phonon intensities are relatively well understood [32] and tractable calculations can be readily carried out [38].

There have been a number of general approaches to the inelastic surface scattering problem that are capable in principle of describing the complete picture of multiquantum exchanges upon collision [39–56], most of which involve semiclassical approximations or at least invoke some form of the trajectory approximation [57–59]. Actual quantitative calculations of the multiquantum scattered intensities for direct comparison with experiment have generally proven to be difficult and cumbersome to carry out.

In this paper we review the formally exact treatment of the general surface scattering problem. We then sequentially apply the trajectory approximation and the semiclassical approximation in order to make the connection with several of the previous theoretical treatments. We show that under conditions in which the multiphonon intensity is dominated by interactions with quanta whose energies and wave vectors are small, conditions which are very broadly applicable, a quick collision approximation can be applied which leads to expressions which are readily calculated. Finally, we show a number of comparisons with recent experiments illustrating the usefulness of this approach.

2. Formal development

The interaction between the atomic projectile and the surface can be described by a Hamiltonian of the form

$$H = H^{\mathrm{p}} + H^{\mathrm{c}} + V, \tag{1}$$

where H^{p} is the Hamiltonian of the free particle, H^{c} is the Hamiltonian of the unperturbed crystal, and V is the interaction coupling the projectile and crystal.

Following the approach of Brako and Newns [43,44] and of Bortolani and Levi [28], it is convenient for considerations of parallel momentum exchange to consider the probability density of exchanging, between particle and crystal, both an amount E of energy and an amount $\hbar K$ of parallel momentum. Such a probability density is defined by

$$P(K, E) = 1/\hbar^2 \langle\langle (n_{\mathrm{i}}, k_{\mathrm{i}}| S^{\dagger} \delta(H^{\mathrm{c}} - E_{\mathrm{i}}^{\mathrm{c}} - E) \times \delta(\hat{K}^{\mathrm{c}} - K^{\mathrm{c}} + K) S | k_{\mathrm{i}}, n_{\mathrm{i}}) \rangle\rangle, \tag{2}$$

where $\hbar\hat{K}^{\mathrm{c}}$ is the momentum operator for the crystal. The differential reflection coefficient, which is usually compared to the experimentally measured intensities, is related to Eq. (2) by a simple density of states:

$$\frac{\mathrm{d}R}{\mathrm{d}\Omega_{\mathrm{f}}\,\mathrm{d}E_{\mathrm{f}}} = \hbar^2 k_{\mathrm{f}} k_{\mathrm{f}z} P(K, E), \tag{3}$$

where $\hbar k_{\mathrm{f}}$ is the final projectile momentum and $\hbar k_{\mathrm{f}z}$ is its component in the direction normal to the surface. The delta functions in Eq. (2) are rewritten as integral representations [60] in the transformation usually ascribed to Glauber [61,62] and Van Hove [63], and after defining time dependent operators in a generalized interaction picture according to

$$S(R, t) = \mathrm{e}^{-\mathrm{i}(R\cdot\hat{K}^{\mathrm{c}} - H^{\mathrm{c}}t/\hbar)} S\, \mathrm{e}^{\mathrm{i}(R\cdot\hat{K}^{\mathrm{c}} - H^{\mathrm{c}}t/\hbar)}, \tag{4}$$

the differential reflection coefficient appears in the general form

$$\frac{\mathrm{d}R}{\mathrm{d}\Omega_{\mathrm{f}}\,\mathrm{d}E_{\mathrm{f}}} = \frac{k_{\mathrm{f}} k_{\mathrm{f}_z}}{(2\pi)^3 \hbar L^2} \int_{-\infty}^{+\infty} \mathrm{d}t \int \mathrm{d}R \int \mathrm{d}R' \times \mathrm{e}^{\mathrm{i}[K\cdot(R-R') - Et/\hbar]} \langle\langle (n_{\mathrm{i}}, k_{\mathrm{i}}| S^{\dagger}(R, 0)| k_{\mathrm{f}}) \times (k_{\mathrm{f}}| S(R', t)| k_{\mathrm{i}}, n_{\mathrm{i}}) \rangle\rangle. \tag{5}$$

Eq. (5) is formally without approximation, and is a quite general expression for describing the scattering. However, in order to make progress towards tractable calculations, approximations must be applied. The scattering operator $S(\alpha)$ can be represented in several forms, but perhaps the most convenient for the later introduction of approximations is the time dependent exponential in the interaction picture [64]

$$S(\alpha) = \mathscr{T} \lim_{t_0 \to \infty} \mathrm{e}^{(-\mathrm{i}/\hbar)\int_{-t_0}^{+t_0} V(\alpha;\tau)\,\mathrm{d}\tau}, \tag{6}$$

where $\alpha = (R, t)$ signifies the supplementary variables of the driving operators as in Eq. (4) and $\mathscr{T}$ is the time ordering operator. When Eq. (6) is inserted into Eq. (5), even very severe approximations applied to the many-body potential V will often give a final result for the scattering probability which still obeys the condition of unitarity. This will be the starting point for further development.

3. Trajectory approximation

The trajectory approximation consists of assuming that the projectile follows a classical trajectory from its initial

state characterized by momentum $\hbar k_i$ to its final state $\hbar k_f$. An alternative way of arriving at the trajectory approximation is to set up the scattering problem in the Feynman path integral formalism, and then limit the number of paths to those which are classically allowed. Although the particle moves along a classical trajectory, it is still possible to consider its further interactions with the crystal, in particular the inelastic exchange of quanta, in a completely quantum mechanical manner. Another useful approximation that has often been applied to inelastic scattering is the semiclassical approximation. The semiclassical approximation has several different forms but usually it consists of imposing the further restriction that the final and initial energies of the projectile are not appreciably different, as expressed by the relation $k_f \approx k_i$.

We will develop the trajectory approximation directly from Eq. (5). We first need to discuss the interaction potential $V = V(\boldsymbol{r}, \{\boldsymbol{u}\})$ where $\{\boldsymbol{u}\}$ symbolizes the set of displacement variables of the crystal. Since the atomic projectiles do not scatter directly from the crystal atoms, rather they are scattered by the weak electron cloud in front of the surface, it may be much more useful to divide the unit cell up into divisions other than those usually associated directly with the atomic cores, and this will become particularly useful when we consider the continuum potential model below.

We write the interaction potential as the sum of two parts

$$V = V^0 + V^1, \tag{7}$$

where the "strong" part V^0 contains the terms which backscatter the projectile and prevent it from penetrating appreciably into the bulk, and the remainder V^1 contains the major terms describing interactions with the lattice vibrations. If the potential is expanded in a Taylor series in the lattice vibrations, then

$$V = V(\boldsymbol{r}, \{\boldsymbol{u}_{j,\kappa}\})|_{u_{j,\kappa}=0} + \sum_{j,\kappa} \boldsymbol{u}_{j,\kappa} \cdot \nabla_{j,\kappa} V(\boldsymbol{r}, \{\boldsymbol{u}_{j,\kappa}\})|_{u_{j,\kappa}=0} + \cdots, \tag{8}$$

where $\nabla_{j,\kappa}$ is the gradient operator with respect to the (j, κ) displacement. We use a notation for the set of indices (j,κ), in which j is a two-dimensional variable that counts unit cells of the surface and κ is three-dimensional and counts elements of the basis set within the unit cell including those in all the layers below the surface. Usually κ counts the crystal atoms making up the basis set of the unit cell, but we note that this does not necessarily need to be the case. The logical choice is to associate V^0 with the leading term of Eq. (8) which is now independent of the displacement and let V^1 be the first order term in the expansion in vibrational displacements. Higher order terms in the expansion of the potential (8) have been shown to be unimportant in the case of atom–surface scattering [65].

Within the above potential model and for a crystal in the harmonic approximation the thermal average in Eq. (5) can now be carried out. For operators linear in the harmonic displacements the commutations are handled with the relation $e^A e^B = e^{A+B} e^{[A,B]/2}$, and $\langle\langle e^A \rangle\rangle = e^{\langle\langle A^2/2 \rangle\rangle}$. The result is

$$\frac{dR}{d\Omega_f\, dE_f} = \frac{\rho k_f m^2 L^4}{(2\pi)^3 \hbar^5 k_{iz}} \sum_G \int_{-\infty}^{+\infty} dt \int d\boldsymbol{R} \int d\boldsymbol{R}' \times e^{i[(K+G)\cdot(R-R') - Et/\hbar]} |\tau_{fi}|^2 \sum_l \times e^{iK\cdot R_l}\, e^{-W(R,k)}\, e^{-W(R',k)}\, e^{2\mathscr{W}_l(R,R',t)} \tag{9}$$

where ρ is the density of surface unit cells. $|\tau_{fi}|^2$ is the form factor in which to lowest order approximation the scattering amplitude τ_{fi} is the off-energy-shell transmission matrix for scattering by a unit cell of the zero order potential V^0 [66,67].

The function $\mathscr{W}_l(\boldsymbol{R}, \boldsymbol{R}', t)$ is a generalized correlation function which only depends on the relative distance l between unit cells. The Debye–Waller exponent is given by the correlation function evaluated at equal positions and times $W(\boldsymbol{R}, k) = \mathscr{W}_{l=0}(\boldsymbol{R}, \boldsymbol{R}, t = 0)$.

Eq. (9) is a quite general expression in which the only major approximations, aside from the harmonic approximation, are the expansion of the interaction potential through linear terms only and the application of the trajectory approximation. The $\boldsymbol{G} = 0$ term of Eq. (9) is essentially identical to the result presented by Bortolani and Levi [28] with two exceptions, we have accounted for the periodicity of the lattice which is recovered after averaging over the initial states of the crystal, and the scattering amplitude τ_{fi} does not depend on the variable $\boldsymbol{R}$. This latter difference is simply due to the choice of separation of the interaction potential into the parts V^0 and V^1; making a different choice in which V^0 contains displacements of the basis elements which distort the unit cell will lead to

$$|\tau_{fi}|^2 = \tau_{fi}^{\dagger}(\boldsymbol{R}) \tau_{fi}(\boldsymbol{R}'), \tag{10}$$

after making a reasonable set of simplifying assumptions [66].

We note here that the spatial integrals over $\boldsymbol{R}$ and $\boldsymbol{R}'$ in the differential reflection coefficient of Eq. (9) can be replaced by integrals over a single unit cell. Translation through a lattice vector such as in the operation $\boldsymbol{R} \rightarrow \boldsymbol{R} + \boldsymbol{R}_l$ simply changes the phase of the displacement vector. The correlation function $\mathscr{W}_l(\boldsymbol{R},\boldsymbol{R}',t)$ depends only on the phase difference, and this phase difference is summed over in Eq. (9). Thus the reduction of the spatial integrals to integrals over single unit cells merely multiplies Eq. (9) by a constant equal to the corresponding density of states.

General theories of inelastic surface scattering based on the powerful S-matrix formalism have been developed earlier by Brenig [50] and by Brako and Newns [43] and even much earlier by Beeby [39]. Eq. (9) is more general than these earlier theories in two aspects, interference in

multiphonon scattering arising from contributions from different surface unit cells is accounted for in the summation over lattice sites, and there is a multiplicative form factor $|\tau_{fi}|^2$ which shows that the scattering from a single unit cell provides an envelope for the overall scattering distribution. For example, the theory of Brako and Newns in the form as developed by Celli and Himes [3,68] is recovered exactly if in Eq. (9) only the term $l = 0$ and $G = 0$ is retained and if $|\tau_{fi}|^2$ is set equal to unity.

4. Quick scattering limit

We now come to the question of extraction the quick collision result out of the more general trajectory approximation of Eq. (9). The quick collision approximation is the assumption that the collision is rapid compared to a typical phonon vibration period. In general, this is not a good assumption, but the multiphonon scattering is expected to be dominated by small frequency and long wavelength vibrational modes, and for these a quick collision is a reasonable assumption. The end result is to produce a correlation function of the simple and well known form

$$\mathscr{W}_l(R, R', t) = \langle\langle k \cdot u_0(R, 0) k \cdot u_l(R', t)\rangle\rangle, \qquad (11)$$

i.e., the time dependent displacement correlation function.

Inserting the approximate form of Eq. (11) into the differential reflection coefficient of Eq. (9) above gives

$$\frac{dR}{d\Omega_f\, dE_f} = \frac{\rho k_f m^2 L^4}{(2\pi)^3 \hbar^5 k_{iz}} \sum_G \int_{-\infty}^{+\infty} dt \int_{u.c.} dR \int_{u.c.} dR' \times e^{i[(K+G)\cdot(R-R') - Et/\hbar]} \times |\tau_{fi}|^2 \sum_l e^{iK\cdot R_l}\, e^{-W(R,k)}\, e^{-W(R',k)} \times e^{\langle\langle k\cdot u_0(R,0) k\cdot u_l(R',t)\rangle\rangle}, \qquad (12)$$

with the Debye–Waller exponent taking on the classic form

$$W_\kappa(k) = \tfrac{1}{2}\langle\langle [k \cdot u_{l,\kappa}(t)]^2\rangle\rangle. \qquad (13)$$

At this point we have spelled out a complete set of approximations necessary to obtain the relatively simple and straightforward form of the differential reflection coefficient Eq. (12) in the quick collision limit. Finally, we note that the reduction of the full trajectory approximation of Eq. (9) to the fast collision approximation of Eq. (12) provides, in the intervening steps, a hierarchy of different stages of approximation which may prove to be useful in special cases.

A particularly useful and simple model for the surface scattering is for a surface which is flat and continuous, rather than made up of a summation of discrete scattering cores. In fact this is the behavior expected for smooth, close-packed metal surfaces. With such surfaces the repulsive part of the atom–surface potential, which contributes most strongly to the inelastic scattering, is due to the Pauli exchange forces between the incoming atomic cloud and the surface electron density. The Smolokowsky smoothing of the decaying tail of the conduction electrons would be expected to provide a very continuous surface potential.

For a continuous, flat surface the Debye–Waller exponent $W(R, k)$ in Eq. (12) no longer depends on the position coordinate R and the correlation function depends only on the difference between its position arguments. Consequently, the spatial integrals can be reduced to a single integral over the surface and the differential reflection coefficient becomes

$$\frac{dR}{d\Omega_f\, dE_f} = \frac{k_f m^2}{(2\pi)^3 \hbar^5 k_{iz} S_{u.c.}} |\tau_{fi}|^2\, e^{-2W(k)} \times \int_{-\infty}^{+\infty} dt \int dR\, e^{i[K\cdot R - Et/\hbar]}\, e^{\langle\langle k\cdot u(0,0) k\cdot u(R,t)\rangle\rangle}. \qquad (14)$$

Eq. (14) embodies the continuum model of the atom–surface interaction. Although approximate, Eq. (14) is a complete quantum-mechanical description of the scattering process. Expansion of $\exp[\langle\langle k\cdot u(0,0) k\cdot u(R,t)\rangle\rangle]$ produces an ordered series in terms of numbers of exchanged phonons with the zero order term being the elastic diffraction contribution. In order to obtain the multiphonon part the elastic and single phonon contributions are subtracted from Eq. (14).

5. Classical limit

The classical limit occurs for high temperatures and large energies (or more precisely, large k). Under classical scattering conditions the Debye–Waller factor is so small that elastic and single phonon peaks are completely suppressed, and only multiple phonon exchanges occur. There have been several recent and interesting treatments of semiclassical and classical trajectory approximations to the multiphonon scattering of atomic and molecular particles at surfaces which have considered the classical limit [3,44,50,52,53]. It is of interest to consider the present theory in this limit as it leads to closed form expressions for the scattering intensities, and gives specific criteria for the validity of the classical limit.

For a lattice of discrete scattering centers in the classical limit the time Fourier transform in Eq. (12) can be evaluated by the method of steepest descents. The scattering becomes completely uncorrelated and only the term $l = 0$ in the sum over lattice sites contributes. The final result is the following differential reflection coefficient:

$$\frac{dR}{d\Omega_f\, dE_f} = \frac{m^2 |k_f|}{8\pi^3 \hbar^5 k_{iz}} |\tau_{fi}|^2 \left(\frac{\hbar\pi}{\omega_0 k_B T}\right)^{1/2} \times \exp\left\{-\frac{(E+\hbar\omega_0)^2}{4 k_B T \hbar \omega_0}\right\}. \qquad (15)$$

The Debye–Waller factor no longer appears explicitly in this expression. The scattering intensity is a Gaussian-like function in the energy exchange E, but shifted to the energy loss side by the energy shift $\hbar\omega_0$ given by

$$\hbar\omega_0 = \hbar^2 k^2/2M, \tag{16}$$

where M is the mass of a crystal atom. However, we note that Eq. (15) is not a true Gaussian function because ω_0 is a function of k. The intensity is limited on the energy loss side by the fact that the projectile may loose no more energy than it had initially, and it is skewed towards the energy gain side by the energy dependence of ω_0. The width of the differential reflection coefficient in energy exchange is roughly $2\sqrt{k_B T\hbar\omega_0}$ in energy units, and the peak amplitude decays with increasing temperature as $(k_B T\hbar\omega_0)^{1/2}$. This behavior of the width and peak intensity of the differential reflection coefficient is understandable in terms of the unitarity condition, which guarantees the equality of the number of scattered particles to the number of incident particles. At higher temperatures the intensity spreads over a larger range of E, consequently in order to preserve the number of particles, the peak intensity must decrease accordingly.

The steepest descent evaluation of Eq. (15) also implies a criterion for the validity of the semiclassical result which is

$$2W(k)/6 \gg 1. \tag{17}$$

This is a very stringent criterion, and is in fact rarely satisfied in typical He-scattering experiments, and often not satisfied even when the projectile is a heavier atom such as Ne or Ar. The average number of phonons exchanged in a collision process is approximately equal to $2W$, thus Eq. (17) implies that for the classical approximation to be valid, a truly large number of quanta must be exchanged. In practice it is found that for $2W < 6$ the differential reflection coefficient differs strongly from Gaussian form and is an increasing, rather than decreasing, function of T. For values of $2W \geq 6$ the Gaussian-like form of Eq. (15) is a reasonable approximation.

Eq. (15) is the classical limit for a point particle scattering from a lattice of scattering centers in the limit in which the projectile scatters from a single surface atom. There is a second classical limit for the case of an incident projectile which interacts with many surface atoms, and the surface can be treated as a continuum. This is the limit that should be applicable in the completely classical case of a projectile that is large compared to the interatomic lattice spacing. This is also expected to be the situation in the case of He scattering from metals because the He atoms are repelled by the electron density which extends outside of the surface and this electron density would appear as a continuum. The continuum classical limit is obtained from Eq. (14) upon evaluating the time and spatial Fourier transforms by the method of steepest descents. The final result is a differential reflection coefficient of the following form:

$$\frac{\mathrm{d}R}{\mathrm{d}\Omega_f\,\mathrm{d}E_f} = \frac{m^2|k_f|}{4\pi^3\hbar^5 k_{iz} S_{u.c.}}|\tau_{fi}|^2 v_R^2 \left(\frac{\hbar\pi}{\omega_0 k_B T}\right)^{3/2} \times \exp\left\{-\frac{(E+\hbar\omega_0)^2 + 2\hbar^2 v_R^2 K^2}{4k_B T\hbar\omega_0}\right\}, \tag{18}$$

where v_R is a characteristic velocity, or weighted average of surface phonon velocities parallel to the surface [43]. There is a clear difference between the two classical limits in Eqs. (15) and (18). In the latter, the temperature dependence of the peak in the inelastic intensity varies as $1/T^{3/2}$ as opposed to $1/T^{1/2}$, and there is the extra Gaussian behavior in parallel momentum exchange.

Eq. (18) with the form factor $|\tau_{fi}|^2$ taken to be constant is essentially the expression developed by Brako and Newns [44] and can be arrived at by purely classical thermodynamical treatments of scattering from an isotropic continuum surface [49]. The present treatment produces a specific expression for the energy shift ω_0 given by Eq. (16), whereas in classical or semiclassical treatments [44,49] it is often chosen to be the Baule expression derived from binary particle collisions, modified by the presence of the attractive well:

$$\hbar\omega_0 \approx \frac{4\mu}{(1+\mu)^2}\left(E_i\cos^2\theta_i + D\right), \tag{19}$$

where $\mu = m/M$ is the ratio of the projectile to surface atom mass, E_i is the incident energy, and D is the depth of the attractive potential well in front of the surface. Eq. (16), evaluated in the semiclassical limit where $k_{fz} \approx k_{iz}$ and $k \approx 2k_{iz}$, is very close to Eq. (19), namely

$$\hbar\omega_0 \approx \frac{4\hbar^2 k_{iz}^2}{2M} = 4\mu E_i\cos^2\theta_i, \tag{20}$$

differing from the Baule expression only in the absence of the denominator of the factor $(1+\mu)^2$. We could readily include the well depth D in our treatment by using the same arguments inherent in Eq. (19), that the attractive part of the particle surface potential is rigid (and consequently does not contribute to inelastic exchange) and is sufficiently smoothly varying that it also does not elastically backscatter an appreciable fraction of the incident particle amplitude [69–71].

An interesting special application of the classical limit is the case of the approach to an equilibrium distribution of a scattered gas arising from a very low energy beam of atoms incident on a very hot surface [72]. In the limit $E_i \ll E_f$ we have for the energy exchange and energy shift

$$E = E_f - E_i \to E_f, \tag{21}$$

and

$$\hbar\omega_0 = \frac{\hbar^2}{2M}(k_f - k_i)^2 \to \frac{m}{M}E_f. \tag{22}$$

The differential reflection coefficient of Eq. (18) then takes the form

$$\frac{dR}{d\Omega_f\, dE_f} \propto T^{-3/2} \exp\left\{\frac{-E_f(1+m/M)^2}{4k_B Tm/M}\right\}. \tag{23}$$

Due to the momentum dependence of the energy shift $\hbar\omega_0$, the Gaussian-like function of the energy exchange is skewed to the point where it becomes an exponential in the final energy of the scattered particle. This can be related to the final energy $\mathscr{E}$ of a crystal atom through the well known expression for the energy exchanged in a two particle collision

$$E_f = 4\mathscr{E}\frac{m/M}{(1+m/M)^2}, \tag{24}$$

leaving the scattered intensity in the form

$$\frac{dR}{d\Omega_f\, dE_f} \propto T^{-3/2}\, e^{-\mathscr{E}/k_B T}. \tag{25}$$

The differential reflection coefficients of Eq. (25) or (23) clearly indicate not only that the incident low energy beam of particles has gained energy in the surface collision, but in addition show that the particles leave the surface with an energy distribution having the exponential dependence of the Maxwell–Boltzmann distribution function.

6. Comparisons with experiment

Experiments on He scattering by crystal surfaces provide many pertinent examples of the application of the multiphonon theory developed in this review. Typical experiments use He energies in the thermal range of 5–100 meV, where the de Broglie wavelength is of the order 0.1–1 Å, and hence the motion of the He projectiles is quantum mechanical. With surface temperatures ranging from T substantially less than the surface Debye temperature Θ_D to several times Θ_D, the inelastic background is characterized by an average number of exchanged quanta $2W(k)$ which ranges from less than unity (the quantum regime) to values of 10 or greater (which, according to Eq. (17) is well into the classical regime).

In order to make quantitative comparisons with experiment, the scattering amplitude τ_{fi}, or more precisely the form factor $|\tau_{fi}|^2$ must be specified. This has been studied in previous work explaining the intensities of single phonon inelastic peaks. Harten et al. [73] have found, through a careful consideration of pairwise summation potentials for the He–surface interaction potential V, that $|\tau_{fi}|^2$ can be expressed as the product of a cutoff function in parallel momentum K and the Mott–Jackson matrix element in the perpendicular momentum:

$$|\tau_{fi}|^2 = e^{-2K^2/Q_c^2} v_{M-J}^2(k_{fz}, k_{iz}). \tag{26}$$

The Mott–Jackson factor v_{M-J} is the matrix element of the one-dimensional potential $v(z) = \exp\{-\beta z\}$ taken with respect to its own distorted eigenstates [74]. The form factor of Eq. (26) has exponential decay in K^2, and the Mott–Jackson factor behaves roughly as an exponential decay in the normal momentum difference $|k_{fz}| - |k_{iz}|$. The two parameters Q_c and β are best known for metal surfaces where, on the basis of comparisons with single phonon scattering intensities, it is found that the cutoff momentum Q_c is around 1 Å^{-1}, while the range parameter β is usually somewhat larger than 2 Å^{-1}. The remaining point to be specified is the model of surface vibrations. For all calculations reported here we have used a Debye phonon distribution.

Of the many laboratories carrying out energy resolved He atom scattering experiments, several have specifically investigated the physical properties of the diffuse inelastic or multiphonon contributions to the scattered distributions. These include the group of Skofronick and Safron at Florida State University [75–78], Comsa et al. at Jülich [79], and several collaborators in the laboratory of Toennies at Göttingen [1,80]. Of these the most extensive and carefully controlled is a series of experiments for He on the Cu(001) surface at energies $E_i > 100$ meV. In these experiments the jet beam of He has an angular resolution of better than 2° and at the incident energies of order 100 meV the energy resolution is $\Delta E_i/E_i < 7\%$. A major constraint on the apparatus is that the detector is at a fixed angle of 95.8° relative to the incident beam, thus for each incident angle the energy distribution of scattered particles can be measured at only a single scattering angle. However, the energy resolution is better than 0.1 meV. The Cu(001) single crystal target is free of adsorbates and defects to better than 1% relative to the number of atoms in the surface layer, and steps on the surface are separated by distances larger than 200 nm. The temperature of the crystal can be varied from 40 to 1200 K.

Fig. 1 shows the total intensity scan (i.e., the total scattered intensity without energy resolution) as a function of the angular deviation $\Delta\theta$ away from the specular position, with negative $\Delta\theta$ corresponding to incident angles closer to normal incidence than the specular angle at $\theta_i = 47.9°$ and an incident energy $E_i = 113$ meV. The different scans are for a range of surface temperatures from 203 to 1002 K. At the lowest temperatures the major experimental feature is a sharp peak at the specular position which sits on top of a small but much broader background peak. This sharp peak is the elastic specular peak and is a quantum mechanical feature, the zero order diffraction peak. As the temperature is increased the elastic quantum peak does not broaden but becomes smaller while

the background increases substantially. At the highest temperature the quantum peak has completely disappeared and there is nothing but the broad background. The highest temperature is an example of diffuse inelastic scattering in the classical limit, and this is supported by the value of the Debye–Waller exponent $2W = 10.8$ which is larger than the classical condition of $2W > 6$ discussed above. The calculations shown in the dashed curves are based on the quantum mechanical theory for a continuum potential of Eq. (14), although at the highest temperature the classical theory of Eq. (18) gives the same results. Importantly, the theory agrees with the diffuse background at all tempera-

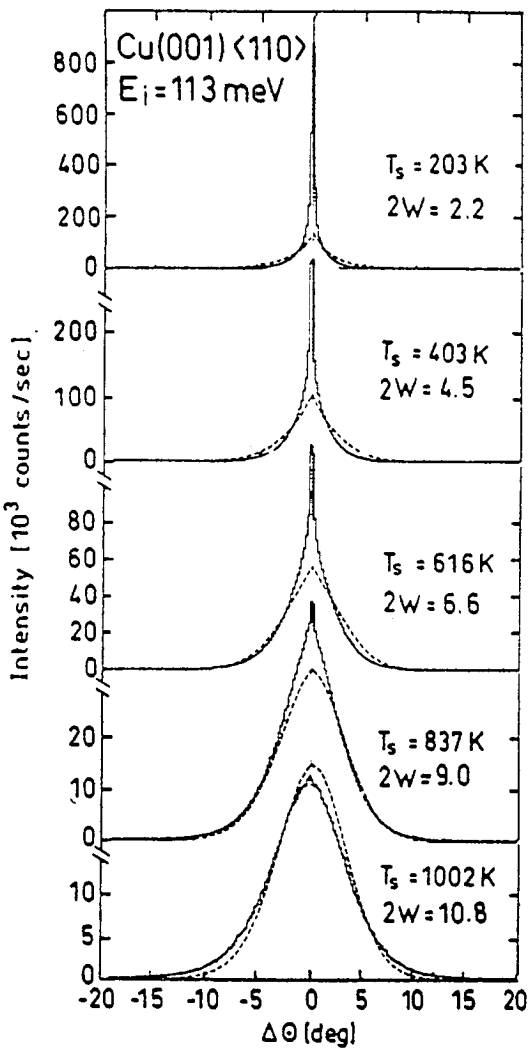

Fig. 1. Total intensity angular scans as a function of the angle of deviation $\Delta\theta$ from the specular position for a range of surface temperatures and an incident energy of 113 meV. The experimental data is shown as a histogram [1] and the theoretical calculation as a dashed line. The experimental apparatus has a fixed angle of 95.8° between incident beam and detector. Elastic and single phonon scattering are not included in the calculation. The values given for $2W$ are evaluated at $\Delta K = 0$ and $\Delta E = 0$.

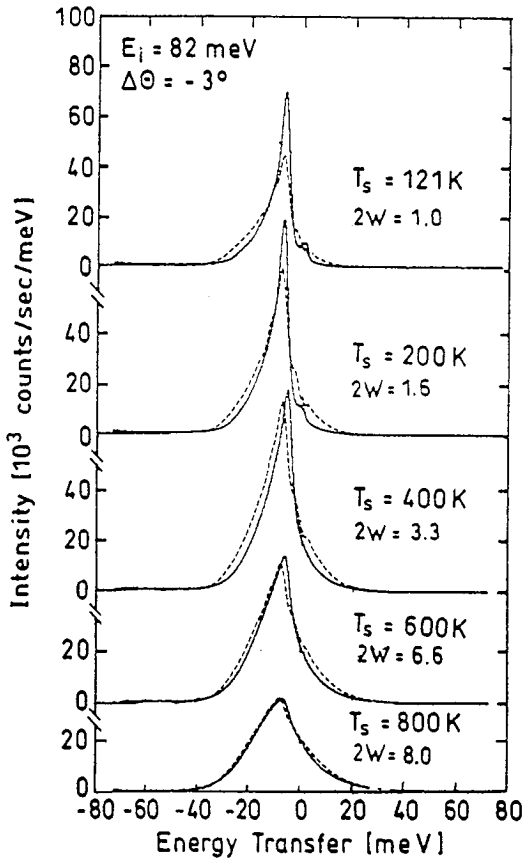

Fig. 2. A series of TOF scans converted to energy transfer for different surface temperatures, with $\Delta\theta = -3°$ and $E_i = 82$ meV [1]. The continuum model theory is the dashed line. The values of $2W$ are evaluated for $\Delta E = 0$.

tures, and agrees very well in the classical regime at the highest temperature. A single set of parameters was used for all calculations reported here, $\beta = 5.7$ Å^{-1}, $Q_c = 2.4$ Å^{-1}, $\Theta_D = 280$ K, and $v_R = 3000$ m/s. These are close to the values $\beta = 3$ Å^{-1}, $Q_c = 1$ Å^{-1} and $\Theta_D = 267$ K obtained from an extensive study of the energy, parallel momentum and temperature dependence of the single phonon intensities from the Cu(001) surface [1]. The value of v_R is slightly larger than the Rayleigh wave velocity for Cu(001).

A more detailed picture of the quantum-to-classical transition emerges in Fig. 2 which shows, as a function of surface temperature, the energy resolved intensity at an incident angle $\theta_i = 44.9°$ ($\theta_f = 50.9°$) and an incident energy of 82 meV. At this angle the scattering is mainly diffuse inelastic with very little indication of sharp quantum mechanical features even for the lowest temperatures. The continuum model calculations, shown by the dashed curves, agree rather well with the measured data, but at the highest temperatures where the scattering is well within the classical regime, the calculations agree nearly perfectly with experiment.

Fig. 3 shows the angular dependence of the scattered intensity in the classical regime. With the surface temperature in the 800 K range and an incident energy of 113 meV, energy resolved scans are shown for a range of incident angles from $\Delta\theta = +3°$ to $\Delta\theta = -12°$. The theoretical calculations are again the dashed lines. We note that, although the angular range of the experimental observations is not large, the intensity varies over a range of three orders of magnitude. The good agreement between theory and experiment over this large range of intensities indicates that the continuum theory does an excellent job of predicting the angular and energy dependence of the intensity of the scattered lobes.

The final example of the validity of our theoretical model is in Fig. 4 which shows not only the transition into the classical scattering regime, but also demonstrates unequivocally that the atom–surface scattering potential must be regarded as a continuum barrier and not as a collection of atomic core scattering centers. Plotted in Fig. 4, as a function of surface temperature, is the maximum peak intensity of the curve for $\Delta\theta = -3°$ in Fig. 3. The experimental points show that at low temperatures the diffuse inelastic intensity grows with increasing temperature, but eventually reaches a maximum after which it decreases with further increase in temperature. The point at which the intensities begin to decrease with further increase of temperature is the beginning of the classical scattering regime. The theoretical calculation based on Eq. (14) shown in the solid curve has the same qualitative form of the experimental points in the low temperature quantum regime, but in the classical regime at $T > 600$ K the agreement with experiment is very good. An extremely interesting result is shown in the dashed curve and the dash-dot curve which show the results of the two purely classical calculations based on Eqs. (15) and (18) respectively. The dashed curve is the $T^{-3/2}$ envelope from Eq. (18) for a continuum surface potential and agrees quite well with the experimental data for $T > 600$ K. The dash-dot curve is the theoretical result for a surface lattice of scattering centers having a $T^{-1/2}$ temperature dependence as in Eq. (15), and this clearly disagrees with experiment. Thus this figure shows not only that the continuum model theory works well, but it also demonstrates conclusively that the metal surface acts as a continuous vibrating barrier.

7. Conclusions

We have presented a brief review of the inelastic scattering of neutral atomic particles from surfaces which is particularly adapted to the description of multiphonon exchanges during the collision. Starting from very general principles of many-body scattering theory, we develop a formal treatment of the scattering problem. However, in order to have a theory tractable enough for calculations, a number of approximations must be made. We apply the trajectory approximation in order to make the connection with earlier treatments of similar problems. We apply a further approximation, called the quick collision approxi-

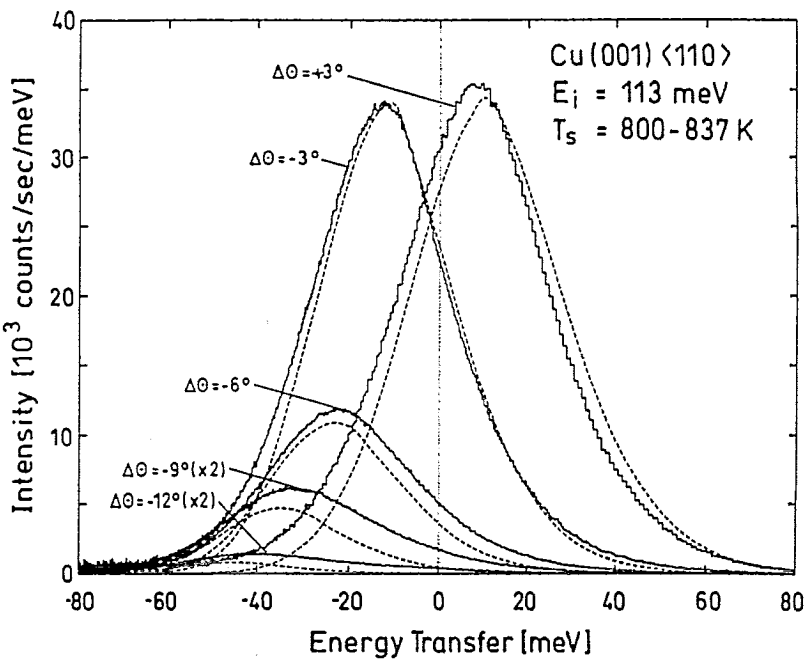

Fig. 3. A series of TOF scans converted to energy transfer for different incident angles from $\Delta\theta = +3°$ to $\Delta\theta = -12°$ for an incident energy of 113 meV [1]. The temperature at $\Delta\theta = +3°$ is 800 K and at all other angles it is 837 K. The theory is the dashed line.

mation, which is particularly useful for carrying out calculations. The quick collision approximation is based on the assumption that the multiphonon part of the scattering intensity is dominated by long wavelength and small frequency phonons.

In order to investigate the correspondence principle transition from the quantum regime to classical scattering, we develop a simple model, called the continuum potential model. In this model the vibrational displacements are assumed to be continuous functions defined over a smooth, flat surface such as would be expected for the interaction of a projectile atom with the exponential tail of conduction electrons extending outside of a metal. This model is used to explore the transition from classical to quantum scattering through comparisons with recent He atom scattering experiments [1] at 100 meV incident energies and substrate temperatures from 100 to 1200 K.

There are two classical limits that result from the theory for large temperatures and high energies, one for the case of a continuum surface and the other for a surface made up of discrete scattering centers. Both of these closed form expressions appear as skewed Gaussian-like functions in the energy exchange with the surface, but they each have a very clear distinguishing signature. The discrete scattering center expression has a temperature dependence of its maximum intensity which varies as $T^{-1/2}$ while the maximum intensity of the continuum surface model varies as $T^{-3/2}$. Comparison with the experiments in the high temperature classical regime shows clearly that the data agrees with the continuum surface model and not at all with the discrete scattering center model.

We have carried out an extensive comparison with experiment for He scattering from a Cu(001) surface, with He incident energies in the 80–120 meV range and surface temperatures of order 100–1200 K. These comparisons include total angular scans as a function of surface temperature, and time of flight energy-resolved scattered intensities as a function of both temperature and incident angle. The agreement is quite good and particularly good in the classical domain. The good agreement achieved between theory and experiment shows that the diffuse multiphonon intensity in atom–surface scattering can be described with

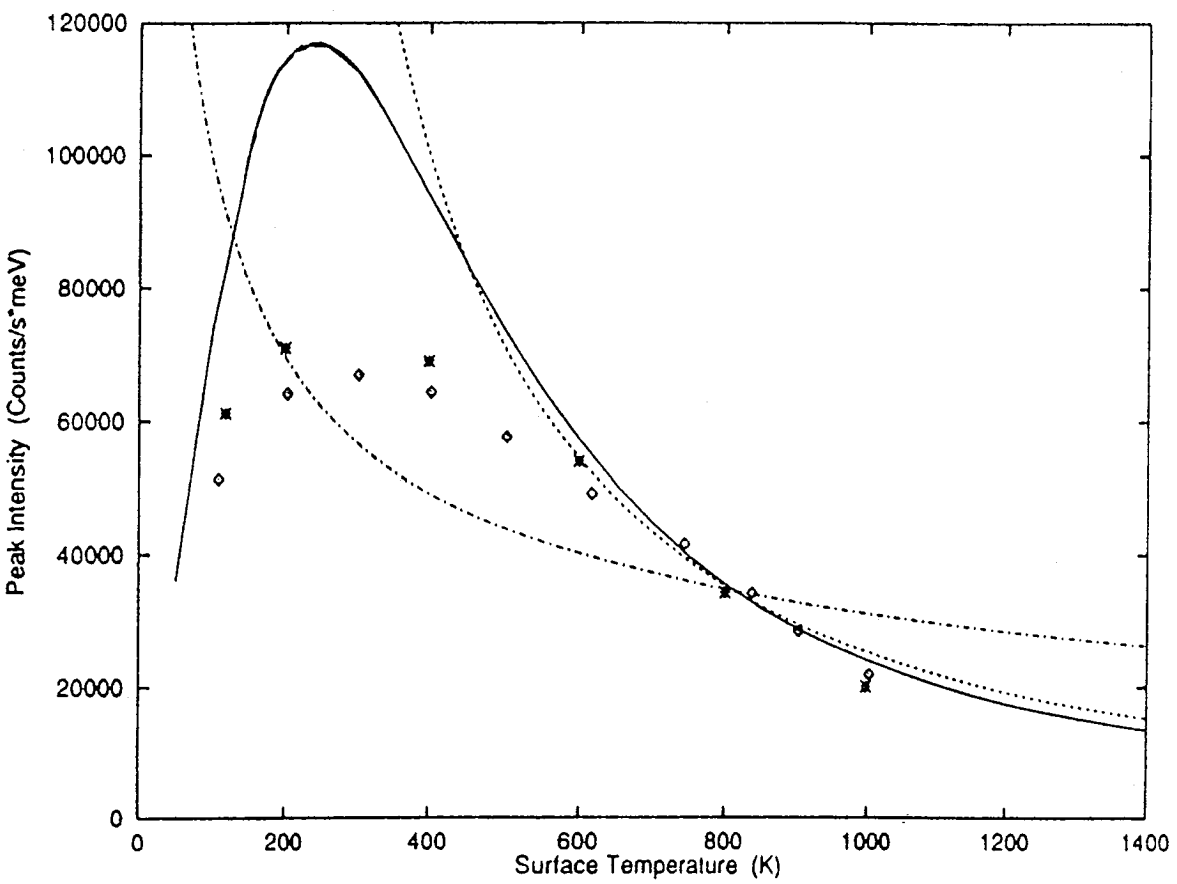

Fig. 4. Maximum peak intensity as a function of surface temperature for the $\Delta\theta = -3°$ incident angle and $E_i = 113$ meV shown in Fig. 3. The two different sets of points are two sets of data taken at different times [1], the solid line is the continuum model theory, the dashed line is the $T_s^{-3/2}$ envelope, and the dash-dot line is the $T_s^{-1/2}$ envelope. The agreement of the experimental data at high T_s with the $T_s^{-3/2}$ envelope demonstrates that the He is scattering from a continuum potential and not from a lattice of discrete centers.

straightforward and tractable calculations. Furthermore, the comparisons with experiment support the two biggest approximations made in the calculations, (i) the use of the quick collision approximation, and (ii) the assumption that the multiphonon intensity does not depend strongly on the details of the phonon spectral density.

This study shows that we have arrived at a basic understanding of the energy exchange process between a colliding atom and a surface in the region where the incident energies are larger than the typical phonon energies but smaller than the energies of typical atomic excitation processes. This work is useful for background subtraction in order to extract from the data reliable values for the intensities of the diffraction and single surface phonon events. The temperature range measured provides a beautiful example of the correspondence transition from the quantum-mechanical regime to classical physics. However, this work also shows that important physical information on the nature of the interaction can be obtained from the diffuse inelastic intensity alone. In particular, comparisons with the data in the classical regime provide clear evidence that the He atoms are scattering from a continuum surface, and this is in accordance with accepted ideas that the incoming atomic projectiles scatter from the asymptotic tail of the electron density extending outward from the last layer of atoms making up the surface. The interaction of the He atoms with the surface vibrations is through the vibrations of the electron density extending outside the surface, and not directly with the vibrations of the underlying crystal atomic cores.

Acknowledgements

The author would like to thank Srilal M. Weera for help with the numerical computations. This work was supported by the NSF under grant No. DMR 9114015.

References

[1] F. Hofmann, J.P. Toennies and J.R. Manson, J. Chem. Phys. 101 (1994) 10155.
[2] J.R. Manson and V. Celli, Phys. Rev. B 39 (1989) 3605.
[3] V. Celli, D. Himes, P. Tran, J.P. Toennies, Ch. Wöll and G. Zhang, Phys. Rev. Lett. 66 (1991) 3160.
[4] O. Stern, Naturwissenschaften 17 (1929) 391.
[5] I. Estermann and O. Stern, Z. Phys. 61 (1930) 95.
[6] I. Estermann, R. Frisch and O. Stern, Z. Phys. 73 (1931) 348.
[7] R. Frisch and O. Stern, Z. Phys. 84 (1933) 430.
[8] J.M. Jackson and N.F. Mott, Proc. R. Soc. London, Ser. A 137 (1932) 703.
[9] J.E. Lennard-Jones and C. Strachan, Proc. R. Soc. London, Ser. A 150 (1935) 442.
[10] C. Strachan, Proc. R. Soc. London, Ser. A 140 (1935) 456.
[11] J.E. Lennard-Jones and A.F. Devonshire, Nature 137 (1936) 1069.
[12] J.E. Lennard-Jones and A.F. Devonshire, Proc. R. Soc. London, Ser. A 156 (1936) 6.
[13] J.E. Lennard-Jones and A.F. Devonshire, Proc. R. Soc. London, Ser. A 156 (1936) 29.
[14] J.E. Lennard-Jones and A.F. Devonshire, Proc. R. Soc. London, Ser. A 158 (1936) 242.
[15] J.E. Lennard-Jones and A.F. Devonshire, Proc. R. Soc. London, Ser. A 158 (1936) 253.
[16] A.F. Devonshire, Proc. R. Soc. London, Ser. A 156 (1936) 37.
[17] A.F. Devonshire, Proc. R. Soc. London, Ser. A 158 (1937) 269.
[18] J.N. Smith, Jr., D.R. O'Keefe, H. Saltzburg and R.L. Palmer, J. Chem. Phys. 50 (1969) 4667.
[19] S.S. Fisher, M.N. Bishara, A.R. Kulthau and J.E. Scott, Jr., Proc. 5th. Symp. on Rarefied Gas Dyn. (1969) p. 1227.
[20] R.B. Subbarao and D.R. Miller, J. Chem. Phys. 51 (1969) 4679.
[21] B.R. Williams, J. Chem. Phys. 55 (1971) 1315.
[22] B.R. Williams, J. Chem. Phys. 55 (1971) 3220.
[23] N. Cabrera, V. Celli and R. Manson, Phys. Rev. Lett. 22 (1969) 396.
[24] A. Tsuchida, Surf. Sci. 14 (1969) 375.
[25] N. Cabrera, V. Celli, F.O. Goodman and R. Manson, Surf. Sci. 19 (1970) 67.
[26] H. Hoinkes, Rev. Mod. Phys. 52 (1980) 933.
[27] G. Boato and P. Cantini, Adv. Electron. Electron Phys. 60 (1983) 95.
[28] V. Bortolani and A.C. Levi, Rivista del Nuovo Cimento 9 (1986) 1.
[29] J.A. Barker and D.J. Auerbach, Surf. Sci. Rep. 4 (1984) 1.
[30] T. Engle and K.H. Rieder, Springer Tracts Mod. Phys. 19 (1982) 1.
[31] R.B. Gerber, Chem. Rev. 87 (1987) 29.
[32] V. Celli, in: Many Body Phenomena at Surfaces, eds. D. Langreth and H. Suhl (Academic Press, New York, 1984) p. 315.
[33] J.P. Toennies, Phys. Scripta T19 (1987) 39.
[34] A. Lahee, J.R. Manson, J.P. Toennies and Ch. Wöll, Phys. Rev. Lett. 57 (1986) 471.
[35] C.W. Skorupka and J.R. Manson, Phys. Rev. B 41 (1990) 8156.
[36] B.J. Hinch and J.P. Toennies, Phys. Rev. B 42 (1990) 1209.
[37] A. Lahee, J.R. Manson, J.P. Toennies and Ch. Wöll, J. Chem. Phys. 86 (1987) 7194.
[38] V. Bortolani, V. Celli, A. Francini, J. Idiodi, G. Santoro, K. Kern, B. Poelsema and G. Comsa, Surf. Sci. 208 (1989) 1.
[39] J.L. Beeby, J. Phys. C 5 (1972) 3438.
[40] J.L. Beeby, J. Phys. C 5 (1972) 3457.
[41] A.C. Levi, Nuovo Cimento B 54 (1979) 357.
[42] A.C. Levi and H. Suhl, Surf. Sci. 88 (1979) 221.
[43] R. Brako and D.M. Newns, Phys. Rev. Lett. 48 (1982) 1859; Surf. Sci. 123 (1982) 439.
[44] R. Brako and D.M. Newns, Surf. Sci. 123 (1982) 439.
[45] M. Lagos, Surf. Sci. 65 (1977) 124.
[46] M. Lagos, Surf. Sci. 71 (1978) 414.
[47] B. Jackson, J. Chem. Phys. 88 (1988) 1383.
[48] B. Jackson, J. Chem. Phys. 92 (1990) 1458.
[49] H.D. Meyer and R.D. Levine, Chem. Phys. 85 (1984) 189.
[50] W. Brenig, Z. Phys. B 36 (1979) 81.
[51] J. Böheim and W. Brenig, Z. Phys. B 41 (1983) 243.

[52] D.A. Micha, J. Chem. Phys. 74 (1981) 2054.
[53] D. Kumamoto and R. Silbey, J. Chem. Phys. 75 (1981) 5164.
[54] M. Jezercak, P.M. Agrawal, C. Smith and L.M. Raff, J. Chem. Phys. 88 (1988) 1264.
[55] R. Kosloff and C. Ceerjan, J. Chem. Phys. 90 (1989) 7556.
[56] B.H. Choi and R.T. Poe, J. Chem. Phys. 83 (1985) 1330.
[57] K. Burke, B. Gumhalter and D. Langreth, to be published.
[58] J.H. Jensen, L.D. Chang and W. Kohn, Phys. Rev. A 40 (1989) 1198.
[59] K. Burke and W. Kohn, Phys. Rev. B 43 (1991) 2477.
[60] R. Weinstock, Phys. Rev. 65 (1944) 1.
[61] R. Glauber, Phys. Rev. 87 (1952) 189.
[62] R. Glauber, Phys. Rev. 98 (1955) 1962.
[63] L. Van Hove, Phys. Rev. 95 (1954) 249.
[64] L.S. Rodberg and R.M. Thaler, Quantum Theory of Scattering (Academic Press, New York, 1967).
[65] G. Armand and J.R. Manson, Phys. Rev. Lett. 53 (1984) 112; G. Armand, C.S. Jayanthi and J.R. Manson, Phys. Rev. B 34 (1986) 6627.
[66] J.R. Manson, V. Celli and D. Himes, Phys. Rev. B 49 (1994) 2782.
[67] J.R. Manson, Phys. Rev. B 43 (1991) 6924.
[68] D. Himes and V. Celli, Surf. Sci. 272 (1992) 139.
[69] J. Beeby, J. Phys. C 4 (1971) L359.
[70] R.I. Masel, Surf. Sci. 77 (1978) L179.
[71] J.R. Manson and G. Armand, Surf. Sci. 184 (1987) 511.
[72] J.R. Manson, Surf. Sci. 272 (1992) 130.
[73] V. Celli, G. Benedek, U. Harten, J.P. Toennies, R.B. Doak and V. Bortolani, Surf. Sci. 143 (1984) L376.
[74] F.O. Goodman and H.Y. Wachman, Dynamics of Gas–Surface Scattering (Academic Press, New York, 1976).
[75] J.G. Skofronick, G.G. Bishop, W.P. Brug, G. Chern, J. Duan, S.A. Safron and J.R. Manson, Superlattices and Microstructures 7, (1990) 239.
[76] J.G. Skofronick, G.G. Bishop, W.P. Brug, G. Chern, J. Duan, S.A. Safron and J.R. Manson, Superlattices and Microstructures 7 (1990) 239.
[77] S.A. Safron, W.P. Brug, G. Chern, J. Duan, J.G. Skofronick and J.R. Manson, J. Vac. Sci. Technol. A 8 (1990) 2627.
[78] G.G. Bishop, W.P. Brug, G. Chern, J. Duan, S.A. Safron, J.G. Skofronick and J.R. Manson, Phys. Rev. B. accepted for publication.
[79] G. Armand and P. Zeppenfeld, Phys. Rev. B 40 (1989) 5936.
[80] F. Hofmann, J.P. Toennies and J.R. Manson, J. Chem. Phys. to be published.